M-2363

J. Chem. Thermodynamics **1989,** 21, 631–651

Heat capacity, thermodynamic properties, and transitions of silver iodide [a]

ROEY SHAVIV, EDGAR F. WESTRUM, JR.,

Department of Chemistry, University of Michigan, Ann Arbor, MI 48109, U.S.A.

FREDRIK GRØNVOLD, SVEIN STØLEN,

Department of Chemistry, University of Oslo, Blindern, Box 1033, 0315 Oslo 3, Norway

AKIRA INABA, HITOSHI FUJII, and HIDEAKI CHIHARA

Department of Chemistry and Chemical Thermodynamics Laboratory, Faculty of Science, Osaka University, Toyonaka, Osaka 560, Japan

(Received 6 February 1989)

The heat capacity of silver iodide was measured using adiabatic calorimetric cryostats over the ranges 7 to 350 K and from 2 to 75 K. The (β to α)- and (β/γ to α)-transitions and the heat capacities of single crystals of β-, of finely divided β/γ-, and of the α-phases were measured in adiabatic calorimetric cryostats and thermostats from 70 to 700 K and from 310 to 523 K. The values of $C_{p,m}$, S°_m, and Φ°_m at 298.15 K are 6.707R, 13.764R, and 8.511R for the β-phase and since the molar volumes of β- and γ-phases are identical and the structures differ only in their stacking sequence, their heat capacities are essentially identical. Moreover, the molar transition-enthalpy increments to the α-phase of the two samples are also equal within the accuracy of the present measurements in spite of the structural differences occasioned by the presence of some γ-AgI in one of them (below the transition temperature). The (partial) enthalpy of the (β/γ to α)-phase transition was found to be $(758.7 \pm 0.8)R \cdot K$ and that of the (β to α)-phase transition was found to be $(758.0 \pm 0.3)R \cdot K$ over the range 405 to 425 K {mean: $(758.4 \pm 0.4)R \cdot K$}. The (total) enthalpy of transition is about $1150R \cdot K$. An abnormal trend in the heat capacity in the low-temperature region was noted. The heat-capacity values are compared with those of prior overlapping measurements by Nernst and Schwers, by Pitzer, and by Madison *et al.* for the β/γ-phase, and in and beyond the transition region with those of numerous prior investigators.

1. Introduction

The polytypes of silver iodide[1] at ambient atmospheric conditions are a hexagonal wurtzite-type structure (β-AgI) coexisting with a cubic face-centered sphalerite-type modification (γ-AgI);[2] however, only the former is thermodynamically stable below 420 K. The conversion rate for the metastable phase is measurable only above 390 K, and the transition does not easily go to completion.[3] At 420 K a first-order phase

[a] Contribution No. 131 from the Chemical Thermodynamics Laboratory, Osaka University.

0021-9614/89/060631+21 $02.00/0

transition yields a body-centered cubic modification (α-AgI)[4] with high ionic mobility and consequent high (ionic) electric conductivity approaching that of a liquid electrolyte.[5]

Numerous reports on the heat capacity of silver iodide by adiabatic calorimetry near the disordering phase transition are extant[6-16] as are $\Delta_{trs}H$ determinations by other methods.

The first heat-capacity determination of β/γ-silver iodide (from 18 to 116 K) is among the very early measurements of Nernst and Schwers[17] and a second—of more recent vintage—from 15 to 300 K by Pitzer.[18] The low end (from 1.8 to 20 K) of the heat capacity was measured more recently by Madison *et al.*[19] In these studies, the temperature dependence at low temperatures was claimed to be at variance with Debye-like trends. These results are confirmed by the present work and are discussed later in this text.

Subsequently Perrott and Fletcher[6-10] observed different heat capacities for samples of different stoichiometry. They found a much higher heat capacity for the stoichiometric α-AgI than for the non-stoichiometric α-AgI over the region 430 to 800 K and an ordering transition with $\Delta_{trs}H^{\circ}_{m} = (151 \pm 25)R \cdot K$ near 700 K. Their results were contradicted by Jost[11] as well as by Nölting and Rein.[16] Perrott and Fletcher found similar phenomena in the heat capacity of silver sulfide.[20] But more recently Grønvold and Westrum[21]—after independent measurements—found no evidence in support of Perrott and Fletcher's observations and hence of their model for disorder. Okazaki and Takano concur.[22]

There are, however, several experimental indications of the onset of an order/disorder phenomenon on the Ag^+ cation sublattice in AgI (675 to 700 K) involving a change in the activation energy for the ionic conductivity noted by Allen and Lazarus,[23] and by Fontana *et al.*,[24] together with a decrease in the α-AgI integrated Raman intensity reported by Mariotto *et al.*[25] The same phenomenon is confirmed in molecular-dynamics simulation studies by Tallon,[26] and even more recently in Brillouin spectra across this region by Börjesson and Torell,[27] revealing changes in the trend of the temperature dependence of the longitudinal and transverse modes as well as in the phonon propagation near the predicted transition temperature. These effects are typical of the Brillouin component on passage through a glass transition. Of the many models used to interpret the intriguing experimental results, a typical one[28] neither implies the existence nor does it exclude the possibility of such a temperature at which the "percolation" in the iodine cage system would be broken. The essential linearity of Lawn's[29] X-ray determined density of the α-phase from 423 to 720 K precludes the presence of a transition.

The temperature-dependent cooperative correlation between occupied silver sites deduced from Raman spectra of Mazzacurati *et al.*[28] was supported through the lattice-gas calculations by Szabo[30] which pointed to the existence of an intermediate partially ordered phase. Further calculations by Szabo and Kertész[31] showed that the self diffusion is strongly anisotropic in the intermediate phase as well as in the ordered low-temperature one.

To resolve all these ambiguities the present authors (on three continents) prepared two distinct samples of silver iodide—one finely divided material a (β/γ-mixture) and

the other a single crystal β-sample—and characterized these by X-ray diffraction and studied their heat capacities, the former from 7 to 350 K (Ann Arbor) and from 310 to 523 K (Oslo) and the latter from (2 to 75 K) and from (70 to 700 K) (both at Osaka). Hence four calorimeters and two samples were employed.

2. Experimental

SAMPLE PROVENANCE AND CHARACTERIZATION

The Oslo sample was made by reacting stoichiometric quantities of 99.99+ mass per cent metallic silver (American Smelting & Refining Co.) and 99.998 mass per cent iodine flakes (Koch-Light Laboraties) in evacuated sealed silica-glass tubes. The yellow powder formed was first heat treated at 370 K for 1 d, and subsequently for 1 d at 410 K, 11 d at 470 K, 1 d at 520 K, 1 d at 570 K, and 11 d at 670 K, before being cooled within the furnace to room temperature.

To get the purest possible β-phase, the Osaka University sample consisted of selected single crystals. Since silver iodide has always proved difficult to grow from solution, a gel method was applied.[32] The process involves diffusion of AgI–HI complexes in solution into an acidic (HI) gel, and the subsequent dissociation of the complex with increasing dilution. The procedures which followed precipitation of fine silver iodide powder from $AgNO_3$ and HI solutions are described elsewhere.[33] The crystals in the gel appeared to be completely clear small hexagonal pyramids up to 3 mm in base diameter, from which the crystals larger than 0.5 mm in size were loaded into the calorimeter vessel. The reagents used were purchased from Wako Pure Chemical Industries, Ltd. The Gel-grown crystals thus obtained are of high-purity stoichiometric β-AgI single crystals without inclusions.[33]

Powder X-ray diffraction photographs at room temperature were taken in an 80 mm diameter Guinier camera with Cu $K\alpha_1$ radiation and silicon as calibration substance; $a(293\ \mathrm{K}) = 543.1065$ pm for Si.[34] Unit-cell dimensions to characterize the samples were derived by the method of least squares using the program CELLKANT.[35]

The Oslo sample consists of a mixture of β- and γ-AgI with cell constants $a = (459.36 \pm 0.07)$ pm and $c = (751.3 \pm 0.2)$ pm, and $a = (649.9 \pm 0.6)$ pm, respectively.† The very weak cubic 331 reflection is the only definite proof of the presence of γ-AgI in the Oslo sample; see table 1. The three strong reflections 111, 220, and 311 overlap with the hexagonal 002, 110, and 112 reflections, respectively. Thus, the hexagonal close packing of the iodine atoms is close to ideal $\{c/a = 1.6356 \approx (8/3)^{1/2}\}$ and the molar volumes of the two close-packed structures $(a_{cub}/a_{hex} = 1.414 \approx \sqrt{2})$ are equal within the limits of error for ideal stoichiometry.

The Osaka sample, even after heating to 700 K and cooling to 2 K, shows the presence of only hexagonal β-AgI with lattice constants: $a = (459.16 \pm 0.05)$ pm, $c = (750.98 \pm 0.20)$ pm.†

The unit cell dimensions obtained agree well with results by Burley[36] $\{a = (459.2 \pm 0.4)$ pm, $c = (751.0 \pm 0.4)$ pm$\}$, by Chateau *et al.*[37] $\{a = (459.24 \pm 0.02)$ pm,

† The uncertainties given for the present results indicate one standard deviation.

TABLE 1. X-ray powder results for the Osaka and the Oslo calorimetric samples of silver iodide, together with calculated $(\sin\theta)^2$ and intensity values of the reflections from the hexagonal and cubic polytypes (Cu $K\alpha_1$ radiation)

AgI (Osaka)		AgI (Oslo)		β-AgI (hexagonal)			γ-AgI (cubic)		
$10^5(\sin\theta)^2$	I	$10^5(\sin\theta)^2$	I	hkl	$10^5(\sin\theta)^2$	I	hkl	$10^5(\sin\theta)^2$	I
3759	1000	3741	305	100	3750	1000			
4213	790	4200	241	002	4201	571	111	4215	1000
4806	516	4801	164	101	4805	652			
—	—	—	—				200	5619	3
7961	226	7955	84	102	7955	343			
11259	981	11259	1000	110	11248	792	220	11239	761
13217	543	13216	155	103	13211	781			
15012	137	15008	85	200	14997	122			
15468	555	15466	552	112	15453	465	311	15453	470
16091	[a]	16095	[a]	201	16048	103			
—	—	—	—	004	16821	2	222	16858	1
19199	55	19190	20	202	19202	76			
—	—	—	—	104	20570	2			
—	—	—	—				400	22477	131
24486	128	24459	72	203	24459	261			
26270	90	26232	37	210	26245	89			
—	—	26677	10				331	26692	203

[a] Coincides with Si-reflection.

$c = 751.04$ pm} and by Wilman[38] {$a = (459.2 \pm 0.2)$ pm, $c = (753.6 \pm 0.2)$ pm} for β-AgI and by Burley[39] {$a = (648.9 \pm 0.5)$ pm}, by Wilman[38] {$a = (648.9 \pm 0.5)$ pm} and by Berry[40] {$a = (649 \pm 2)$ pm} for γ-AgI.

In an attempt to determine the relative amounts of β- and γ-AgI in the Oslo sample, intensities of the reflections on the Guinier photographs were calculated by the program LAZY-PULVERIX.[41] For the hexagonal structure the coordinates and isotropic temperature factors derived by Burley[36] were used. The results are given in table 1. The agreement between observed intensities for presumably pure β-AgI (Osaka) and those calculated is fair. According to Burley,[36] the displacement model with the silver atoms in the tetrahedral-bond directions is not supported by the experimental results. Further attempts by Burley[36] to improve the agreement between his observed and calculated structure factors and corrections for anomalous dispersion, led only to a slight improvement of the R-factor from 8.0 to 6.6 per cent. A more recent refinement attempt by Cava *et al.*[42] by neutron diffraction did not bring the R-factor below 6.5 per cent. The lack of agreement was ascribed in part to inadequacy of the extinction correction used.

In the present intensity calculations for cubic γ-AgI, the sphalerite or zinc-blende type structure was assumed. The results show that the 331 reflection should have considerable intensity. It is, however, very weak in the Oslo sample, and indicates that β-AgI dominates. Superposed reflections from β- and γ-AgI with their calculated intensities do not yield the intensities observed for the Oslo sample. Whether this is occasioned by incorrect structural models, preferred orientation, anomalous absorption, or other phenomena is not yet known. Crushing the Osaka crystals does,

however, lead to intensity relations similar to those reported for the Oslo sample in table 1. Furthermore, the intensity relation in the Oslo sample was found to vary somewhat with heat treatment.

CALORIMETRIC TECHNIQUE

The cryogenic heat-capacity measurements at Ann Arbor were made in the Mark X adiabatic cryostat, which has been described previously.[43] The sample was contained in a gold-plated copper calorimeter (laboratory designation W-139). The calorimeter had a mass of 13.21 g and an internal volume of 23 cm^3. The temperature of the calorimeter was measured with a Leeds & Northrup platinum-encapsulated resistance thermometer in an entrant well. The thermometer was calibrated by the U.S. National Bureau of Standards against IPTS-68 and is considered to reproduce the thermodynamic temperature scale within 0.03 K from 5 to 300 K.

About 71.9 g of sample were put into the calorimeter. This corresponds to about 0.3 mol; 234.7727 $g \cdot mol^{-1}$ was selected as the molar mass of AgI. To facilitate rapid thermal equilibration 2.03 kPa at 300 K of helium gas was introduced after evacuation. The calorimeter was then sealed, placed in the cryostat, and cooled. The heat capacity of the empty calorimeter represented 10 per cent of the total heat capacity at temperatures below 50 K and became about 25 to 30 per cent at higher temperatures.

The heat-capacity measurements at Osaka University were made with two adiabatic calorimeters; one was employed for measurements between 2 and 75 K and the other between 70 and 700 K. Although both have been described already,[44,45] new calorimetric vessels were used and will be described elsewhere.[46] The IPTS-68 temperature scale was used for two platinum resistance thermometers above 13.81 K and the helium vapor-pressure scale and a gas-thermometric scale were used for a germanium resistance thermometer below 15 K. The mass of the sample loaded was 17.6 g for both measurements. The heat capacity of the empty calorimeter in the Osaka experiment, represented 35 per cent at 3 K decreasing to 11 per cent at 10 K and gradually increasing from 26 to 70 per cent of the total heat capacity between 20 and 70 K for the low-temperature cryostat. For the high-temperature cryostat at Osaka the heat capacity of the empty calorimeter was between 63 per cent and 74 per cent over the entire temperature range of the experiment (70 to 700 K).

The high-temperature calorimetric apparatus and measuring technique at Oslo have already been described in detail.[47] The computer-operated calorimeter was intermittently heated and was surrounded by electrically heated and electronically controlled adiabatic shields. The sample was enclosed in an evacuated and sealed silica-glass tube of about 50 cm^3 volume, tightly fitted into the silver calorimeter. A central entrant well in the tube served for the heater and platinum resistance thermometer. The resistance-thermometer was calibrated locally, at the ice, steam, tin, and zinc points. Temperatures are judged to correspond with IPTS-68 to within 0.08 K.

The heat capacity of the empty calorimeter was determined in a separate series of experiments and was about 45 per cent of the total with a standard deviation of a

TABLE 2. Molar heat capacities of silver iodide ($R = 8.3144\ J \cdot K^{-1} \cdot mol^{-1}$; $M(AgI) = 234.7727\ g \cdot mol^{-1}$)

T/K	$C_{p,m}/R$	T/K	$C_{p,m}/R$	T/K	$C_{p,m}/R$	T/K	$C_{p,m}/R$	T/K	$C_{p,m}/R$
Low-temperature measurements—University of Michigan									
Series I		138.91	5.836	257.79	6.480	9.06	0.794	37.75	3.168
282.48	6.613	144.03	5.878	262.97	6.506	9.95	0.912	39.62	3.299
289.04	6.653	149.16	5.915	268.15	6.533	10.86	1.023	41.58	3.432
295.57	6.684	154.31	5.949	273.33	6.559	11.80	1.125	43.64	3.565
302.09	6.725	159.48	5.984	278.51	6.588	12.75	1.220	45.80	3.701
308.61	6.765	164.64	6.016	283.69	6.622	13.71	1.311	48.08	3.835
315.13	6.804	169.80	6.045	288.87	6.652	14.67	1.404	50.47	3.968
321.65	6.843	174.97	6.074	294.06	6.677	15.65	1.487	55.38	4.215
328.17	6.885	180.14	6.101	299.24	6.706	16.73	1.572	58.29	4.349
334.68	6.931	185.31	6.126			17.90	1.660	61.29	4.476
341.20	6.981	190.48	6.152	Series III		19.08	1.747	64.79	4.608
346.54	7.014	195.65	6.178	8.79	0.755	20.34	1.841	68.78	4.737
		200.83	6.202	9.74	0.885	21.73	1.942	72.79	4.853
Series II		206.00	6.226	10.64	0.998	23.10	2.046	76.81	4.965
93.73	5.326	211.18	6.250	11.57	1.100	24.47	2.150	80.84	5.075
98.71	5.393	216.36	6.275	12.52	1.198	25.78	2.249	85.37	5.187
103.59	5.461	221.53	6.300	13.47	1.289	27.06	2.347	90.42	5.279
108.40	5.527	226.71	6.325	14.44	1.383	28.40	2.450	95.50	5.349
113.34	5.594	231.89	6.350	15.41	1.469	29.80	2.558	100.58	5.420
118.45	5.651	237.07	6.376			31.27	2.674	105.67	5.493
123.57	5.703	242.25	6.402	Series IV		32.74	2.789	110.76	5.559
128.70	5.747	247.43	6.427	7.41	0.536	34.29	2.909	116.12	5.626
133.80	5.794	252.61	6.452	8.20	0.667	35.98	3.038		
High-temperature measurements—University of Oslo									
Series V		489.72	6.882	$\Delta_{trs}H_m$ Detn. B		Series VII		453.05	6.890
374.06	7.208	498.39	6.878	422.88	6.938	326.15	6.850	458.61	6.890
382.39	7.310	507.07	6.866	430.10	6.926	338.59	6.942	464.19	6.882
390.67	7.392			438.63	6.930	350.98	7.028	469.78	6.858
398.92	7.514	Series VI		450.50	6.920	363.28	7.140	475.39	6.870
$\Delta_{trs}H_m$ Detn. A		315.20	6.806	462.44	6.908	375.51	7.260	484.44	6.872
429.57	6.920	327.05	6.868	474.46	6.882	387.67	7.392	497.10	6.862
438.11	6.916	338.84	6.944	486.56	6.858	399.37	7.558	509.83	6.838
446.67	6.922	350.59	7.034	498.77	6.830	$\Delta_{trs}H_m$ Detn. C		522.61	6.848
455.24	6.904	362.29	7.140	510.90	6.844	430.76	6.896		
463.83	6.892	373.83	7.260	523.04	6.818	436.35	6.904		
472.45	6.884	385.36	7.328			441.92	6.902		
481.08	6.894	396.87	7.438			447.49	6.892		
High-temperature measurements—Osaka University									
Series I		90.894	5.274	116.926	5.619	144.868	5.863	173.839	6.041
69.645	4.760	92.915	5.308	119.213	5.642	147.200	5.881	176.339	6.057
71.522	4.815	94.963	5.338	121.511	5.665	149.549	5.899	178.845	6.068
73.385	4.871	97.041	5.362	123.823	5.687	151.914	5.910	181.374	6.083
75.254	4.920	99.148	5.392	126.159	5.711	154.286	5.926	183.912	6.097
77.142	4.967	101.283	5.426	128.494	5.730	156.670	5.938	186.457	6.111
79.050	5.023	103.445	5.454	130.842	5.751	159.071	5.955	189.010	6.124
80.980	5.082	105.637	5.483	133.189	5.771	161.492	5.967	191.562	6.140
82.931	5.126	107.866	5.516	135.521	5.791	163.933	5.984	194.120	6.153
84.904	5.169	110.118	5.541	137.852	5.810	166.397	5.998	196.679	6.166
86.902	5.210	112.379	5.570	140.195	5.828	168.868	6.012	199.241	6.181
88.899	5.244	114.648	5.595	142.538	5.849	171.343	6.027	201.812	6.193

TABLE 2—*continued*

T/K	$C_{p,m}/R$	T/K	$C_{p,m}/R$	T/K	$C_{p,m}/R$	T/K	$C_{p,m}/R$	T/K	$C_{p,m}/R$
204.389	6.206	303.780	6.749	$\Delta_{trs}H_m$ Detn. A'		484.033	6.871	617.936	6.792
206.976	6.222	306.631	6.770	425.637	6.967	487.498	6.862	621.589	6.791
209.603	6.234	309.479	6.789	428.787	6.954	491.269	6.865	625.235	6.804
212.209	6.246	312.331	6.806	431.263	6.942	494.766	6.863	628.879	6.786
214.825	6.259	315.176	6.828	433.946	6.937	498.277	6.857	632.515	6.794
217.443	6.275	318.028	6.845	436.958	6.927	501.808	6.858	636.150	6.799
220.054	6.283	320.886	6.863	440.021	6.919	505.375	6.858	639.821	6.794
222.668	6.298	323.744	6.880	443.141	6.912	508.982	6.854	643.458	6.801
225.311	6.312	326.604	6.904	446.265	6.918	512.631	6.854	647.080	6.804
227.987	6.322	329.468	6.924	449.393	6.904	516.335	6.846	650.704	6.785
230.679	6.337	332.337	6.946	452.526	6.904	520.091	6.839	654.325	6.792
233.399	6.352	335.206	6.958	455.672	6.900	523.890	6.829	657.941	6.812
236.153	6.366	338.076	6.978	458.831	6.899	527.726	6.828	661.554	6.799
238.978	6.388	340.940	7.006	462.002	6.899	531.598	6.826	665.159	6.813
241.760	6.400	343.799	7.026	465.188	6.894	535.514	6.821	668.764	6.812
244.553	6.414	346.663	7.049			539.448	6.818	672.367	6.812
247.348	6.426	349.533	7.076	Series II		543.612	6.822	675.965	6.813
250.145	6.442	352.405	7.097	422.635	6.919	547.599	6.816	679.557	6.835
252.944	6.453	355.280	7.123	425.666	6.918	551.622	6.810	683.148	6.826
255.737	6.467	358.150	7.145	428.713	6.917	555.681	6.806	686.742	6.845
258.533	6.484	361.025	7.167	431.786	6.922	559.781	6.809	690.321	6.838
261.331	6.495	363.905	7.186	434.887	6.913	563.920	6.810	693.902	6.838
264.139	6.508	366.780	7.219	438.022	6.918	568.094	6.811	697.488	6.835
266.958	6.525	369.657	7.242	441.193	6.917	570.247	6.811	701.070	6.860
269.781	6.546	372.538	7.269	444.384	6.917	573.931	6.815		
272.608	6.566	375.412	7.301	447.581	6.908	577.615	6.799	Series III	
275.439	6.575	378.281	7.339	450.800	6.902	581.298	6.807	$\Delta_{trs}H_m$ Detn. B'	
278.275	6.597	381.153	7.372	454.052	6.902	584.975	6.807		
281.106	6.610	384.026	7.399	457.309	6.902	588.652	6.813	Series IV	
283.938	6.625	386.895	7.439	460.573	6.898	592.325	6.809	$\Delta_{trs}H_m$ Detn. C'	
286.772	6.643	389.758	7.475	463.856	6.894	595.993	6.801		
289.600	6.661	392.615	7.511	467.175	6.884	599.658	6.809	Series V	
292.432	6.675	395.465	7.535	470.507	6.889	603.320	6.798	T_{trs} Detn.	
295.268	6.693	398.307	7.582	473.857	6.875	606.976	6.807		
298.103	6.711	401.144	7.630	477.225	6.871	610.630	6.801		
300.939	6.735	403.976	7.655	480.610	6.870	614.286	6.793		
				Low-temperature measurements—Osaka University					
Series VI		7.289	0.502	15.106	1.426	33.018	2.811	55.770	4.224
2.430	0.007	7.702	0.563	15.904	1.488	34.507	2.926	57.314	4.297
2.762	0.011	8.129	0.626	16.890	1.567	36.013	3.041	58.859	4.362
3.018	0.016	8.597	0.694	17.941	1.659	37.507	3.160	60.407	4.425
3.221	0.024	9.134	0.765	18.946	1.744	39.009	3.269	61.956	4.490
3.431	0.034	9.829	0.871	19.972	1.815	40.514	3.372	63.508	4.552
3.701	0.051	10.054	0.964	21.105	1.897	42.025	3.470	65.063	4.600
4.031	0.077	11.178	1.045	22.229	1.981	43.538	3.562	66.619	4.656
4.415	0.116	11.878	1.119	23.368	2.067	45.054	3.655	68.177	4.716
4.819	0.156	12.612	1.190	24.553	2.156	46.575	3.750	69.737	4.765
5.233	0.210	13.379	1.259	25.837	2.254	48.099	3.838	71.300	4.815
5.652	0.265	14.196	1.352	27.234	2.361	49.628	3.919	72.863	4.860
6.064	0.323			28.665	2.470	51.158	4.003	74.429	4.901
6.465	0.381	Series VII		30.121	2.583	52.692	4.077	75.995	4.947
6.876	0.437	14.412	1.368	31.556	2.697	54.230	4.147		

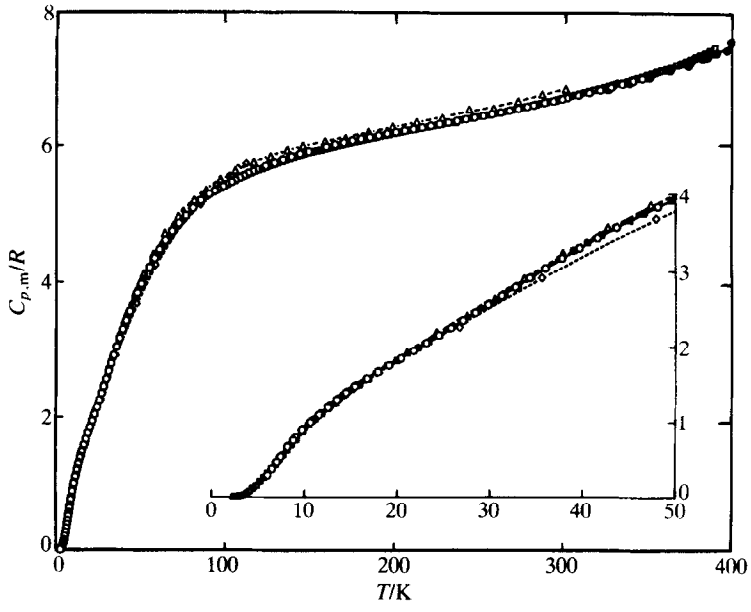

FIGURE 1. Subambient molar heat capacity of silver iodide: ○, This research (U. of Michigan); ●, This research (U. of Oslo); □, This research (Osaka University); △, Pitzer;[18] ◇, Nernst and Schwers;[17] ——, Madison *et al.*[19]

single measurement from the smoothed heat capacity curve of about 0.15 per cent. Small corrections were applied for differences in mass of the silica-glass containers. The mass of the sample used was about 161.2 g.

3. Results

ANALYSIS OF RESULTS

The lower-temperature heat capacities for AgI are listed in table 2 and plotted in figures 1 and 2. The results of the low-temperature Ann Arbor and Osaka experiments agree within experimental error with the heat capacity reported by Madison *et al.*[19] for the very low end over the common range of measurement. Both the Osaka and the Ann Arbor results are in good accord over the range 7 to 350 K as shown on the above plot of figure 2 (see also Section 4). The experimental results reported here are about 2 per cent below the heat capacity reported for AgI by Pitzer.[18] We confirm the presence of a "small wave" and the non-Debye behavior between 7 and 20 K, that was reported earlier, as an abnormally high contribution (figure 1, inset).

The entropy and the enthalpy were evaluated by extrapolation of the heat-capacity curve to zero temperature and integrating. The experimental results for both the Osaka and the Oslo samples were averaged and then fitted to three polynomial segments: one of order 13 from 2.5 to 50 K, a second of order 15 from 46

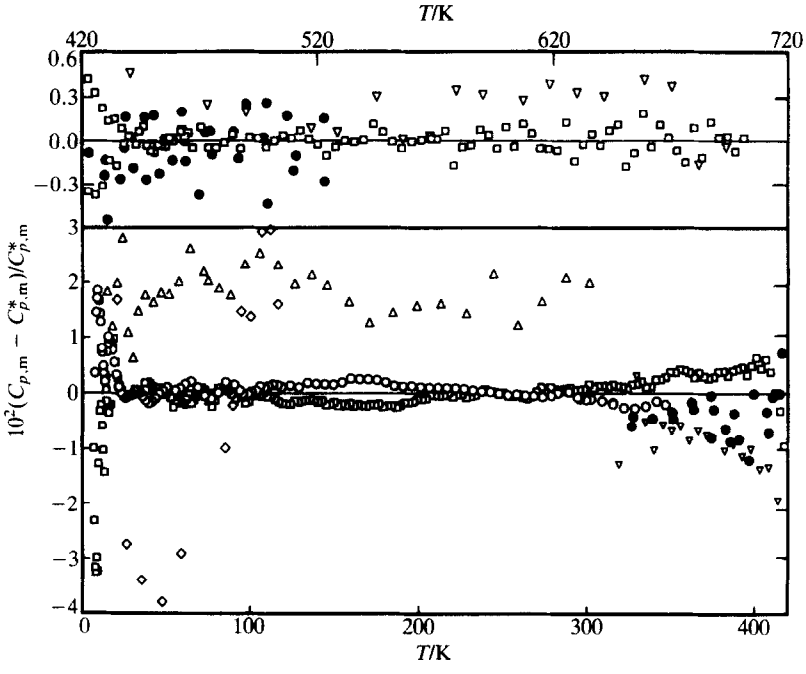

FIGURE 2. Deviations $(C_{p,m} - C^*_{p,m})/C^*_{p,m}$ from smooth curve ($C^*_{p,m}$ represents smooth values generated by the FITAB2 computer program from the mean value on the Osaka and the Oslo samples): ○, this research (U. of Michigan); ●, this research (U. of Oslo); □, this research (Osaka University); △, Pitzer;[18] ◇, Nernst and Schwers;[17] ▽, Nölting and Rein.[48]

to 170 K, and a third of order 11 from 160 to 420 K. There were at least three points of overlap between two neighboring segments and three artificial points at the extremities. The extrapolation from 2.4 K to zero included the experimental values reported by Madison *et al.*,[10] and the resulting entropy increment $\{S^\circ_m(T) - S_m(0)\}$ and enthalpy increment $\{H^\circ_m(T) - H^\circ_m(0)\}$ are $0.391R$ and $2.890R \cdot K$ at 10 K. The corresponding values at 298.15 K are $13.764R$ and $1566.4R \cdot K$.

The higher-temperature experimental results (table 2 and figure 3) were fitted to one polynomial segment of order 13 from 422 to 700 K. The results were found to be in excellent accord with those of Nölting and Rein[16] for the α-phase above 430 K. In the transitional region the heat capacity was estimated from large-scale plots and integrated manually. The (partial) transitional evaluations are given in table 3. A horizontal cut with $C_{p,m} = 7.603R$ was used as background level from 405 to 420.0 K, whereas one with $C_{p,m} = 6.922R$ was used from 420.0 to 425 K (see Section 4). The thus defined (partial) transitional enthalpy and entropy were calculated from determinations A and C, giving $\Delta^{425\,K}_{405\,K} H^\circ_m = (758.7 \pm 0.8)R \cdot K$ and $\Delta^{425\,K}_{405\,K} S^\circ_m = (1.814 \pm 0.018)R$. Determination B was not included due to the very long stabilization periods used, which makes the temperature drift during the experiments more important. The three Osaka determinations (table 3) are in close accord and their mean value is $(758.0 \pm 0.3)R \cdot K$. Hence, the (overall) mean is $(758.4 \pm 0.5)R \cdot K$.

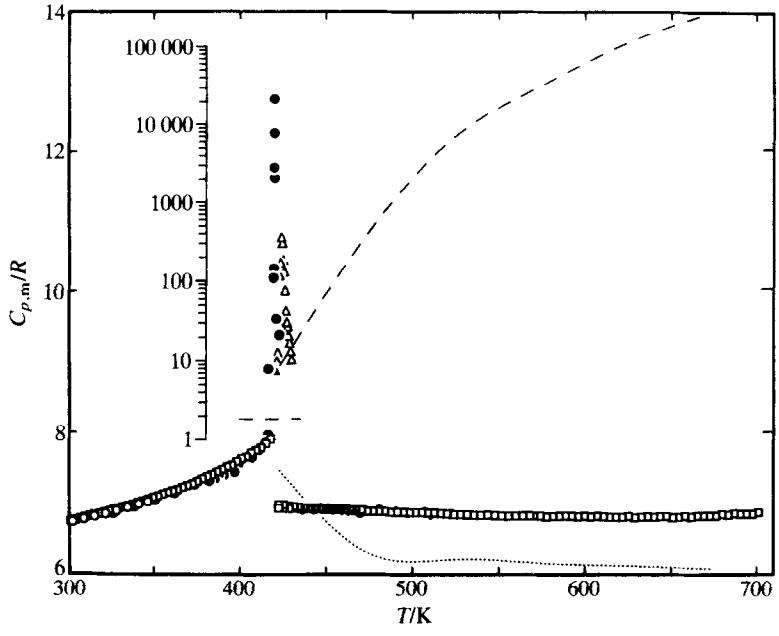

FIGURE 3. Superambient molar heat capacity of silver iodide: ○, this research (U. of Michigan); ●, this research (U. of Oslo); □, this research (Osaka University); – – –, Perrott and Fletcher,[7] "stoichiometric" AgI; · · ·, Perrott and Fletcher,[7] "nonstoichiometric" AgI. (The logarithmic scale corresponds only to the transition region.)

The higher-temperature derived thermodynamic values based on the smoothed values are also given in table 4 at selected temperatures.

4. Discussion

THE SUB-AMBIENT HEAT CAPACITY

The results of this experiment were about 2 per cent lower than the results of similar measurements by Pitzer[18] (figure 2) using isoperibol calorimetry. The deviations of Pitzer's points are shown on the same curve and the points are seen to be relatively less precise. Our measurements, however, form a very smooth curve with very small deviations throughout the region. Results of the determination of the heat capacity of silver iodide by Nernst and Schwers[17] are lower than those of this study by 1 to more than 3 per cent for measurements below 90 K and are higher to about the same extent between 90 and 117 K (figure 2). Avogadro *et al.*[49] published an approximation for the heat capacity of silver iodide by subtracting the heat capacity of $Ag_2O \cdot 2B_2O_3$ from that of $(AgI)_{0.5}(Ag_2O \cdot 2B_2O_3)_{0.5}$. The reliability of their results is such as to make their values consistent with both Pitzer's and our values and thus they cannot serve as a basis for judgment. At the very low end our results agree very well with a previous measurement by Madison *et al.*;[19] their results however overlap with Pitzer's over only a small temperature range.

TABLE 3. (Partial) enthalpies of transition of silver iodide; stabilization times τ
($R = 8.3144\ \mathrm{J \cdot K^{-1} \cdot mol^{-1}}$; $M(\mathrm{AgI}) = 234.7727\ \mathrm{g \cdot mol^{-1}}$)

T / K	ΔT / K	$C_{p,m}/R$	$C_{p,m(non\text{-}trs)}/R$	τ / min	$\Delta_{exc}H/R \cdot K$	T_2 / K
		High-temperature measurements		University of Oslo		
$\Delta_{trs}H_m$	Detn. A					
407.118	8.1810	7.646	7.603	56	0.35	411.208
414.979	7.8530	7.859	7.603	106	2.01	419.061
419.622	1.1230	143.5	7.491	151	152.83	420.184
420.193	0.0214	8280	6.922	146	177.08	420.206
420.210	0.0080	22100	6.922	73	177.15	420.214
420.256	0.0840	2097	6.922	74	175.63	420.298
422.800	5.0015	21.617	6.922	64	73.50	425.300
				$\Delta^{425\,K}_{403.027\,K}H^\circ_m$:	758.55	
				$\Delta^{425\,K}_{405\,K}H^\circ_m$:	758.41	
$\Delta_{trs}H_m$	Detn. B					
408.311	11.379	7.638	7.603	69	0.41	414.012
416.437	4.8985	7.969	7.603	287	1.79	418.887
419.364	0.9545	108.9	7.603	287	96.71	419.841
419.862	0.0420	2822	7.603	310	118.43	419.883
419.889	0.0110	21600	7.603	720	237.77	419.894
419.909	0.0307	7725	7.603	787	236.71	419.925
421.103	2.3559	34.20	6.944	339	64.20	422.281
424.878	5.1944	6.937	6.922	178	0.11	427.475
				$\Delta^{425\,K}_{402.609\,K}H^\circ_m$:	755.97	
				$\Delta^{425\,K}_{405\,K}H^\circ_m$:	755.79	
$\Delta_{trs}H_m$	Detn. C					
410.79	12.096	7.739	7.603	70	1.64	416.851
419.59	5.5220	144.4	7.310	208	756.84	422.373
425.16	5.5980	7.029	6.922	70	0.60	427.971
				$\Delta^{425\,K}_{404.756\,K}H^\circ_m$:	759.09	
				$\Delta^{425\,K}_{405\,K}H^\circ_m$:	759.06	
Oslo mean value of Detns. A and C $\Delta_{trs}H^\circ_m = (758.7 \pm 0.8)R \cdot K$						
		High-temperature measurements—Osaka University				
$\Delta_{trs}H_m$	Detn. A′					
406.800	2.8201	7.712	7.603		0.31	408.211
409.618	2.8141	7.748	7.603		0.41	411.026
412.428	2.8078	7.785	7.603		0.51	413.833
415.232	2.7991	7.844	7.603		0.67	416.632
418.026	2.7907	7.904	7.603		0.84	419.422
420.389	1.9344	397.3	7.089		754.77	421.356
422.784	2.8556	6.973	6.922		0.08	424.212
				$\Delta^{425\,K}_{405.39\,K}H^\circ_m$:	757.59	
				$\Delta^{425\,K}_{405\,K}H^\circ_m$:	757.60	
$\Delta_{trs}H_m$	Detn. B′					
420.381	1.8274	420.4	7.081		755.24	421.295
				$\Delta^{421.295\,K}_{419.468\,K}H^\circ_m$:	755.24	
				$\Delta^{425\,K}_{405\,K}H^\circ_m$:	758.07	
$\Delta_{trs}H_m$	Detn. C′					
420.375	1.8708	411.0	7.096		755.55	421.310
				$\Delta^{425\,K}_{405\,K}H^\circ_m$:	758.38	
Osaka mean value of $\Delta_{trs}H^\circ_m = (758.0 \pm 0.3)R \cdot K$						
Mean value of $\Delta_{trs}H^\circ_m = (758.4 \pm 0.4)R \cdot K$						

TABLE 4. Thermodynamic properties at selected temperatures for silver iodide
($R = 8.3144\ J \cdot K^{-1} \cdot mol^{-1}$; $M(AgI) = 234.7727\ g \cdot mol^{-1}$)

T / K	$C^\circ_{p,m}/R$	$\Delta_0^T S^\circ_m/R$	$\Delta_0^T H^\circ_m/R \cdot K$	Φ°_m/R	T / K	$C^\circ_{p,m}/R$	$\Delta_0^T S^\circ_m/R$	$\Delta_0^T H^\circ_m/R \cdot K$	Φ°_m/R
				Phase β					
0	0	0	0	0	170	6.031	10.207	751.0	5.789
3	0.019	0.004	0.011	0.001	180	6.089	10.553	811.6	6.044
5	0.177	0.044	0.178	0.008	190	6.142	10.884	872.8	6.290
8	0.610	0.217	1.337	0.050	200	6.191	11.200	934.5	6.528
10	0.904	0.391	2.890	0.102	210	6.239	11.503	996.6	6.758
15	1.420	0.863	8.796	0.276	220	6.287	11.795	1059.2	6.980
20	1.807	1.325	16.875	0.481	230	6.337	12.075	1122.4	7.196
25	2.191	1.770	26.871	0.695	240	6.389	12.346	1186.0	7.405
30	2.574	2.203	38.782	0.910	250	6.441	12.608	1250.1	7.608
35	2.965	2.629	52.63	1.125	260	6.493	12.862	1314.8	7.805
40	3.331	3.049	68.39	1.340	270	6.545	13.108	1380.0	7.997
45	3.652	3.461	85.86	1.552	280	6.599	13.347	1445.7	8.183
50	3.939	3.861	104.86	1.763	290	6.657	13.579	1512.0	8.366
60	4.417	4.623	146.75	2.177	298.15	6.707	13.764	1566.4	8.511
70	4.771	5.332	192.77	2.578	300	6.718	13.806	1578.9	8.543
80	5.054	5.988	241.94	2.964	325	6.883	14.350	1748.9	8.969
90	5.264	6.596	293.60	3.334	350	7.053	14.866	1923.0	9.372
100	5.412	7.159	347.01	3.689	375	7.275	15.36	2101.9	9.755
110	5.543	7.681	401.79	4.028	400	7.567	15.84	2287.4	10.120
120	5.661	8.168	457.83	4.353	405	7.603	15.93	2325.3	10.189
130	5.752	8.625	514.9	4.664	410	7.603	16.03	2363.3	10.266
140	5.836	9.054	572.8	4.963	415	7.603	16.12	2401.3	10.334
150	5.911	9.460	631.6	5.249	420	7.603	16.21	2439.3	10.402
160	5.971	9.843	691.0	5.524					
				Phase α[a]					
420	6.922	18.02	3199.6	10.402	550	6.810	19.87	4091.2	12.431
425	6.922	18.10	3232.3	10.495	600	6.803	20.46	4431.6	13.074
450	6.908	18.50	3405.2	10.932	650	6.797	21.01	4771.3	13.670
475	6.877	18.87	3578.5	11.336	700	6.850	21.51	5112.	14.207
500	6.859	19.22	3749.5	11.721					

[a] Assuming an isothermal transition.

The agreement between the heat-capacity values for the Osaka sample and the Oslo sample is good only below 100 K and in the α-phase. The heat capacity of the Osaka sample is lower than that of the Oslo sample between 100 and 300 K, and is higher between 300 and 420 K (see figure 2). These deviations are slightly larger than experimental error and might be due to the different thermal histories of the samples. The Osaka sample on which the subambient measurements were made was synthesized by a gel method and was heated only to 700 K. The Oslo sample was synthesized at high temperatures and was annealed before the measurement. After annealing of the Osaka sample at 700 K essentially identical heat capacities were obtained on both samples below 70 K (see table 2 for thermal history).

The $C_{p,m}/R$ curve (figure 1) is nearly linear from 10 to 50 K. The $C_{p,m}/RT$ against T^2 curve (figure 4) rises sharply at temperatures lower than 8 K and levels off to

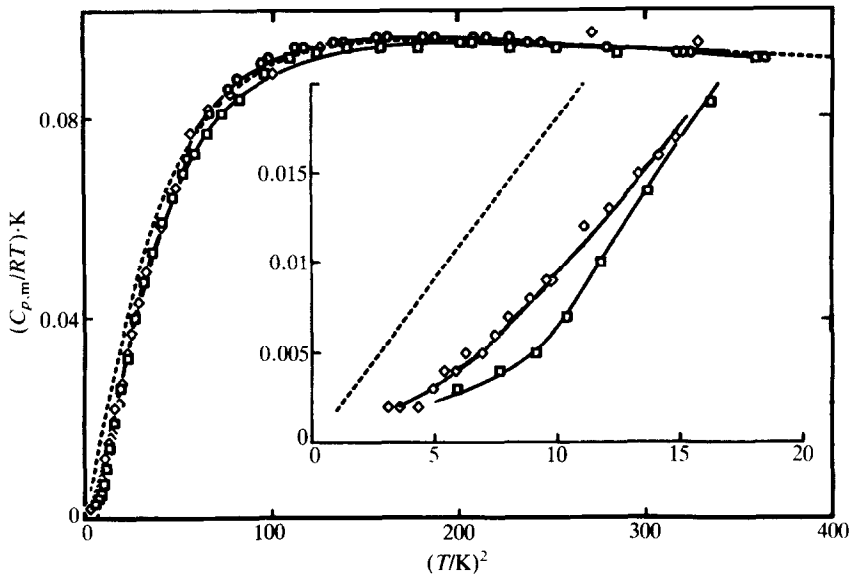

FIGURE 4. $C_{p,m}/RT$ against T^2 for silver iodide: ○, this research (U. of Michigan); □, this research (Osaka University); ◇, Madison *et al.*;[19] – – –, calculated using the LEM-2 program based on $\Theta_{KW} = 34$ K.

nearly a constant value between 10 and 20 K indicating that the heat capacity rises almost linearly with temperature over the region. Above 20 K, $C_{p,m}/RT$ gradually decreases by 5 per cent between 20 and 30 K by 8 per cent between 30 and 50 K. An early explanation[18] of this phenomenon suggests a severely anharmonic five-minima potential function for the silver ions.[50] However, a potential function with a single minimum at the center of the tetrahedron of iodide ions was subsequently developed by Cava *et al.*[42] and X-ray diffractional evidence for such a function was provided by Burley.[36].

This "non-Debye" behavior results from a "non-Debye" phonon density of states $g(\omega)$ as shown by Bührer *et al.*[51] who used a density-of-states function that was derived from the experimental phonon-dispersion relations measured by inelastic neutron scattering. The lattice heat capacity based on this density-of-states function agrees well with our experimental results below 60 K. Above 60 K deviation of C_p from C_V becomes significant.

The apparent Θ_D in the region below 60 K varies several fold. (At higher temperatures Θ_D drops to zero when the heat capacity exceeds the Dulong and Petit limit.) Between 7 and 50 K a computer-aided approximation to represent the temperature dependence of the heat capacity based on a several-parameter phonon-distribution function[52] yielded a characteristic temperature (Θ_{KW}) which is constant (figure 5) indicating that a good approximation to $g(\omega)$ has been achieved. An attempt to extend this approximation below 7 K, using the heat capacity reported by Madison *et al.* yielded a sharp upward trend in Θ_{KW} as well as in Θ_D. We note that change in Θ_D is much larger than in Θ_{KW}. We also note that the experimental

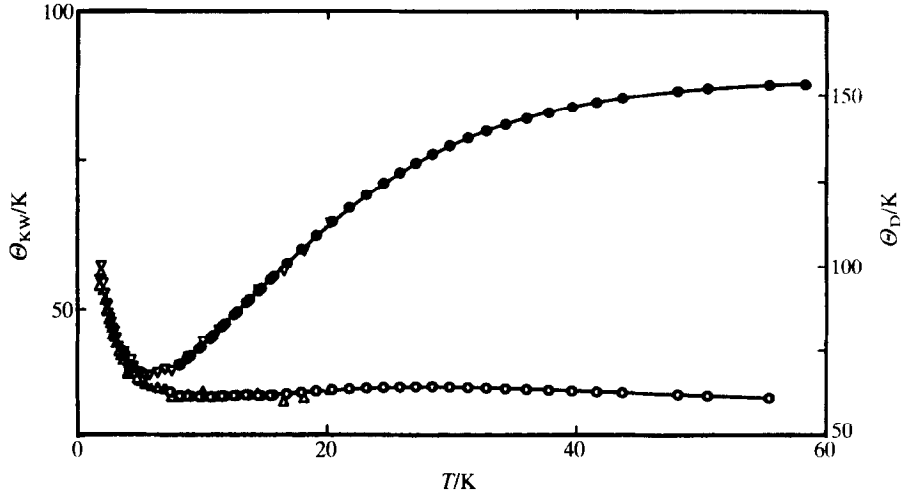

FIGURE 5. Apparent characteristic temperatures Θ_D and Θ_{KW} for silver iodide: (a) Θ_{KW}: ○, this research (U. of Michigan); △, Madison *et al.*[19] (b) Θ_D: ●, this research (U. of Michigan); ▽, Madison *et al.*[19] The Osaka points (which agree well) are not shown to avoid an even greater density of points.

heat-capacity values are significantly lower than those predicted by both the theoretically approximated and the experimental[51] phonon distribution of states, and are closer to the values predicted by the theoretical approximation. The fact that the experimental heat capacity is lower than the heat capacity predicted both by the experimental distribution function and the theoretical approximation—Θ_{KW}—provides a convincing argument for the absence of any special contribution—such as the sought precursor indication of the fast ion state[19]—in the heat capacity.

THE SUPER-AMBIENT HEAT CAPACITY—ENTHALPY OF TRANSITION

The experimentally determined heat capacity of silver iodide can, to a first approximation, be represented by a sum of three contributions:

$$C_{obs} = C_V + C_d + C_{trs}.$$

Here C_V is a constant-volume heat capacity in the harmonic approximation, arbitrarily calculated using a (constant) Debye temperature (taken as the maximum of Θ_D—equal to 150 K—in a plot of Θ_D against temperature). A calculated $C_d = TV\alpha^2/\kappa$ accounts for anharmonic vibrations, whereas C_{trs} represents the premonitory contribution to the structural-disordering phase transition taking place near 420 K.

The constant Debye temperature is in good agreement with that calculated from elastic constants.[53] The dilational contribution was estimated using the temperature dependence of the molar volume V_m and the isobaric expansivity α obtained by Lieser[54] in the temperature range 5 to 420 K. The isothermal compressibility

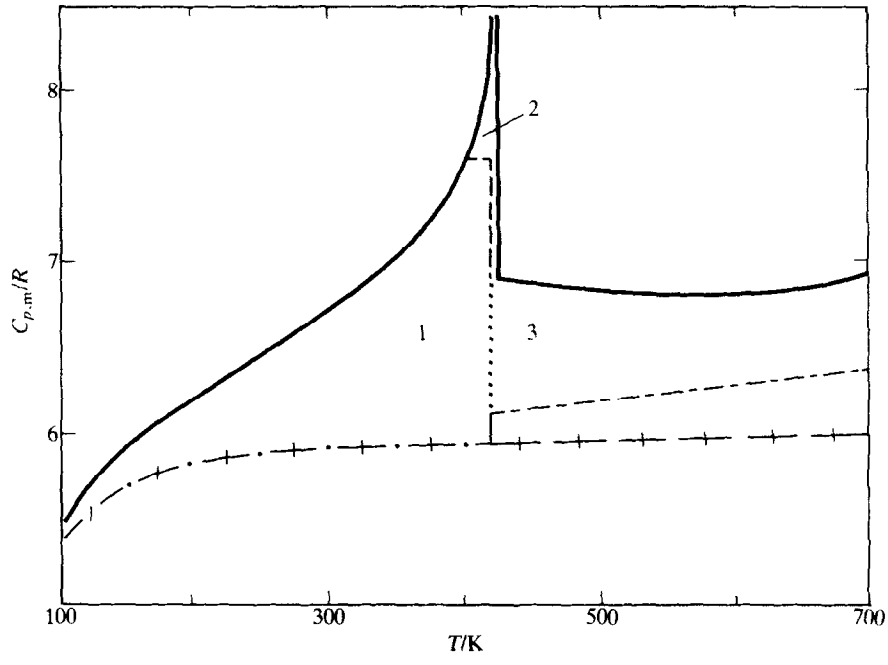

FIGURE 6. Resolution of the heat capacity of silver iodide. + + +, $C_{V,m}$; — · —, $C_{p,m}$ (lattice); ——, observed $C_{p,m}$; 1, "pre-transitional" area ($221R \cdot K$); 2, transitional area ($759R \cdot K$); 3, "post-transitional" area ($165R \cdot K$).

$\kappa = 4.0 \times 10^{-11}$ Pa^{-1}, obtained for the β-phase[55] at ambient temperature was assumed to be valid (and is essentially confirmed by the value 4.17×10^{-11} Pa^{-1} at 295 K).[56] With identical molar volumes and differences only in the stacking sequences, the γ- and β-AgI have practically the same heat-capacity behavior and transition temperature. Nölting and Rein[16] reported both transition temperatures to be the same within ±0.5 K, whereas Weiss[57] reported 417.7 K for the (β to α)-transition and 420.2 K for the (γ to α)-transition, but Yamada[58] and Hoshino[13] reported the reverse: (421 to 409 K, respectively). In the α-phase region the expansivity results by Lawn[29] were used together with compressibilities derived from the elastic-constant determinations by Börjesson[59] and by Börjesson and Torell[60] ($\kappa = 7.41 \times 10^{-11}$ Pa^{-1} at 613 K). The thus calculated contributions to the heat capacity are given in figure 6. At low temperatures the very small value of the expansitivity gives a negligible dilational contribution.

The present interpretation implies a more gradual transition than assumed previously. The continuous disordering process gives rise to an appreciable "pre-transitional" heat-capacity contribution—which is clearly perceptible at 100 K (see figure 6)—and a correspondingly high fraction of the transitional enthalpy, $220.8R \cdot K$, in the range 100 to 420 K (Area 1, figure 6) after subtraction of the more cooperative part of the transition (Area 2, figure 6). The low-temperature process, which results in a continuously increasing mole fraction of "defects", may at a given

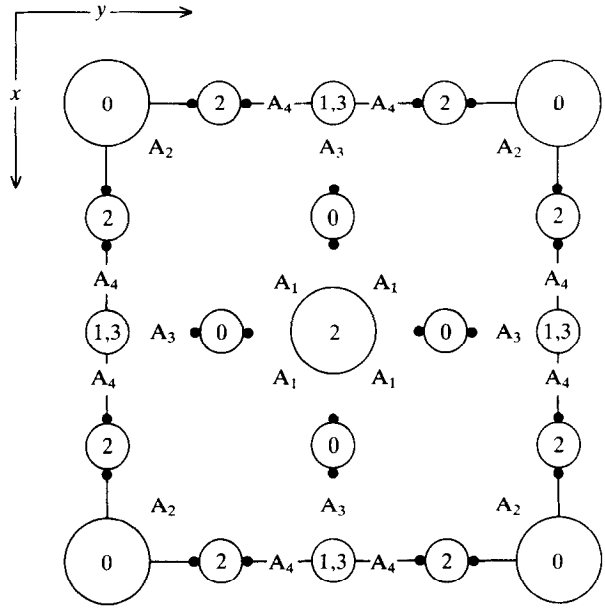

FIGURE 7. Projection of the α-phase structure in the *xy*-plane, with alternative Ag^+ positions indicated. Large circles represent I^- ions in positions 2a 0, 0, 0; 1/2, 1/2, 1/2; of space group Im3m. The *z* parameters are expressed as *z*/4. Small circles represent Ag^+ ions in tetrahedral centers 12d with *z*/4 parameters indicated. The 6b positions are centered between the 12d positions. The 24g displaced tetrahedral positions are indicated by ● when displaced in the *x* or *y* directions—with *z* unchanged, but are not indicated when displaced in the *z* direction. The 24h triangularly coordinated positions are indicated by A_1 ($z = 0$), A_2 ($z = 1/2$), A_3 ($z = 0.11$ and 0.89), and A_4 ($z = 0.39$ and 0.61).

defect mole fraction trigger a first-order transition mechanism.[61,62] The partial enthalpy determinations given in table 3, hence, represent only the more cooperative part of the order-disorder process. In addition, a considerable "post-transitional" enthalpy contribution, $165R \cdot K$, originates from decay of short-range order and exitation of soft modes, linearly extrapolated above the transition temperature in the range 420 to 695 K. The total enthalpy of transition, over the entire range in which excess contribution is present, is $1150R \cdot K$, whereas the corresponding entropy is $2.872R$.

The structure of α-AgI was described by Strock[63] in terms of random distribution of the two Ag^+ ions in the unit cell over 30 positions, and in the latter[63] over 42 positions in the space group Im3m (No. 229). In this structure (see figure 7) the Ag^+ ion in positions 6b (0, 1/2, 1/2; *etc.*) are octahedrally surrounded by the I^- ions in 2a (0, 0, 0; 1/2, 1/2, 1/2), while the Ag^+ ions in 12d (1/4, 0, 1/2; *etc.*) are tetrahedrally surrounded, and those in 24h (0, *y*, *y*; *etc.* with $y = 0.39$) are triangularly surrounded by I^- ions. The correctness of this model was adhered to by Hoshino,[13] while later powder neutron-diffraction studies by Bührer and Hälg[64] discredited the Strock model in favor of the Ag^+ ions being located at displaced tetrahedral 24g sites (x, 0, 1/2; *etc.*, with $x = 0.193$). The different alternatives were reconsidered in the single-crystal neutron-diffraction study by Cava *et al.*[42] and the alternative with all

Ag^+ ions residing in the tetrahedrally coordinated 12d positions with large anharmonic vibrations was found to agree best with the experimental results. The same conclusion was deduced by Hoshino *et al.*[65] from a powder neutron-diffraction study as well as upon reconsideration of the earlier X-ray results[13] in light of the EXAFS study by Boyce *et al.*[66] This study showed that the Ag^+ ion distribution was about 10 pm from the tetrahedral center and displaced toward a tetrahedral face. Furthermore, the residence time of the Ag^+ ions in the displaced tetrahedral site is roughly 3 times the flight time between different tetrahedra at 470 K. Thus, the early conclusions about position and dynamics of the Ag^+ ions from X-ray[1,2,13] and neutron-diffraction[64] studies were found to be inconsistent with the EXAFS results.

Accordingly, the disordering of the Ag^+ ions in the α-AgI phase concerns configurations formed by distributing N Ag^+ ions over $6N$ tetrahedral sites. It is further argued by Beyeler *et al.*[67] that since the phonon frequencies do not change much from the β- to the α-phase, and that the disorder is negligibly small in the β-phase, the transitional entropy is mainly given by the disorder entropy of the α-phase. The limiting entropy increment is then $R \cdot \ln 6$ for AgI, or $1.79R$. Unrestricted disorder of the Ag^+ ions is unattainable, however, as the nearest Ag^+ tetrahedral neighbor sites are only 179 pm apart.

An important result of the present study is that a considerable local structural-disorder entropy accumulates in β-AgI before it transforms to α-AgI (amounting to about $0.7R$ over the range 100 to 420 K). Thus, our estimate of the structural-disorder entropy in α-AgI considerably exceeds the limiting disorder entropy already at 425 K by $0.7R$. Part of the reason may be ascribed to differences in bonding energy of β- and α-AgI, but the fact remains that the Ag^+ ions are structurally largely disordered, and little additional structural disorder entropy will be acquired by further redistribution of the Ag^+ ions.

Comparison with 18 previously published enthalpy-of-transition determinations are given in table 5. The difference between "total" and "partial" transitional functions are seen in figure 6 as the sum of Areas 1, 2, and 3 for which the respective $\Delta_{trs}S_m$s are $0.7R$, $1.81R$, and $0.30R$.

It should be noted that the (β/γ to α)-transition does not occur at a well defined temperature, but depends slightly on the previous thermal history of the sample. Thus, the transition temperature for the Oslo sample in $\Delta_{trs}H_m$ (Detn. A) is about 0.3 K higher than in $\Delta_{trs}H_m$ (Detn. B) for the same fraction transformed.

DEFECT MODELS

Several models for analyzing the excess heat capacity have been proposed. According to Jost,[81]

$$\Delta_{def}C_{p,m}T^2 = \{\exp(\Delta_{def}S_m/2R)\}\{(\Delta_{def}H_m)^2/2R\} \cdot \exp(-\Delta_{def}H_m/2RT).$$

Hence, by plotting $\lg(\Delta_{def}C_{p,m}T^2)$ against $1/T$, the enthalpy and entropy of defect formation are easily found, giving $\Delta_{def}H_m = 250R \cdot K$ and $\Delta_{def}S_m = 0.91R$, as the mean values over the range 250 to 400 K. The change in slope indicates that more

TABLE 5. (Partial) enthalpy of the 420 K disordering phase transition (β/γ to α)-AgI

$\frac{T}{K}$	$\frac{\Delta_{trs}H_m^{\circ}}{R \cdot K}$	Method	Authors	Year
423	740	Drop calorimetry	Bellati and Romanese[68]	1882
418	805	Drop calorimetry	Mallard and Le Chatelier[69]	1883
418	681	Clapeyron	Bridgman[70]	1915
419.8	639	e.m.f.	Cohen and Joss[71]	1928
	749 ± 15		Hennicke[72]	1938
422.5	760	Adiabatic calorimetry	Lieser[12]	1954
421	770	Adiabatic calorimetry	Hoshino[13]	1957
419.7	610 ± 70	Clapeyron	Majumdar[73]	1958
419.7	610 ± 70	Clapeyron	Majumdar and Roy[74]	1959
420.4	712	Adiabatic calorimetry	Nölting[15]	1963
419	760 ± 50	d.t.a.	Rao and Rao[75]	1966
420	780 ± 25	d.t.a.	Berger *et al.*[76]	1967
423	760 ± 50	Adiabatic calorimetry	Perrott and Fletcher[6]	1968
423	755	Drop calorimetry	Carré *et al.*[77]	1969
421	740 ± 35	Adiabatic calorimetry	Nölting and Rein[16]	1969
419	1010	d.t.a.	Natarajan and Rao[78]	1970
	729	d.s.c.	Mellander *et al.*[79]	1981
421	650 ± 250	e.m.f.	Quoranta and Bazán[80]	1983
420.0	758.7 ± 0.8	Adiabatic calorimetry	Present work (Oslo)	1989
420.0	758.0 ± 0.3	Adiabatic calorimetry	Present work (Osaka)	1989

than one defect-formation process is taking place. The observed defect-formation enthalpy is only 25 per cent of that calculated by Jost *et al.*[14] and only 19 per cent of that claimed by Nölting and Rein.[16] This is due at least in part to the different choice of non-transitional heat-capacity curves. In the present evaluation a physical approximation is used, giving $C_{(\text{non-trs})} = C_V + C_d$. In the earlier investigations, the non-transitional heat capacity was extrapolated from experimental $C_{p,m}$ values[14,16] closer to the transition temperature. Thus transitional contributions were considered only in a narrow range near the transition temperature. The presently obtained small value of $\Delta_{def}H_m$ might imply the presence of a "large" fraction of defects even below the order-disorder temperature—in agreement with the appreciable ionic conductivity in the same temperature range.

The present interpretation of the excess heat capacity is based on the classical concept of atomic diffusion in solids, where a diffusing ion traverses a barrier with height given by the activation energy. A basic assumption is then that the time spent on a lattice site is much greater than the time spent between the potential-energy minima. However, it has been shown that the probability of finding mobile ions at saddle-point positions is large in fast ionic conductors (see *e.g.* reference 82). Hence, the applicability to the present compound of the normal jump model, where atoms take well defined sites, is doubtful.

THE REPORTED 700 K TRANSITION

As may be noted in figure 6 a significant post-transitional heat-capacity contribution appears to be present. Fontana *et al.*'s[21] Raman spectra show a pronounced

decrease over the range 590 to 650 K interpreted by Mariotto *et al.*[22] as further disordering or "melting" of the silver sublattice. Brillouin spectra determinations by Börjesson and Torell[59] confirm abrupt changes in the trend of the temperature dependence of the longitudinal-mode frequencies near 650 K (although the transverse-mode frequencies are unaffected) attributed to redistribution of silver ions from tetrahedral to trigonal and octagonal sites yielding an isotropic distribution. Mazzacurati *et al.*[28] proposed also that near 700 K the distribution of silver ions becomes homogeneous and isotropic. The model of Huberman and Martin[83] on pseudospin densities involves redistribution among energetically equivalent sites whether or not crystallographically equivalent. The observation of Börjesson and Torell[60] favors a redistribution which also includes the jumping of silver ions between equivalent tetrahedral and non-equivalent trigonal and octahedral sites.

Modelers tend to relate their interpretations to the cooperative transition near 700 K reported by Perrott and Fletcher[6-10] as involving $(151 \pm 25)R \cdot K$ of isothermal transitional enthalpy plus an additional approximately $1500R \cdot K$ "excess" inter-transitional enthalpy {between the (β to α) and 700 K transitions}. However, a total enthalpy increment of this magnitude is too great to be reconciled with the further disordering of silver ions or with the calorimetric results of this research and that of others[14,16,48] (see figure 3) on the magnitude and trend of the heat capacity between the (β to α)-transition and melting. The post-(β/α)-transitional enthalpy of this research approximates $63R \cdot K$ (Area 3, figure 6) over the range 425 to 700 K and corresponds more reasonably to theoretical entropy-increment estimates. The present observations indicate disorder corresponding to a transitional entropy increment of $R \cdot \ln 12$, *i.e.* distribution on about 24 positions in the unit cell. Further population of 24 sites requires only $0.69R$, while Perrott and Fletcher's[6-10] additional transition gives about $2R$! The approximately constant trend of our heat capacities above the (β to α)-transition (actually gently concave upwards) probably involves a decrease in post-transitional disordering contribution plus the growing size of the contribution related to the softening in the 700 K region and to premelting contribution at increasing temperatures.

The assistance of Norikazu Komada with the lower-temperature calorimetric measurements at Ann Arbor and with the theoretical calculations, the assistance of Bjørn Lyng Nielsen with the preparation of the Oslo sample and in the higher-temperature calorimetric measurements, that of Curator Gunnar Raade of the Mineralogical-Geological Museum of the University of Oslo for the sample of iodyrite (jodargyrite), and that of Professor Dr J. Nölting, for provision of unpublished experimental heat-capacity values are gratefully acknowledged.

REFERENCES

1. Mellander, B.-E.; Bowling, J. E.; Baranowski, B. *Physica Scripta* **1980,** 22, 541.
2. Burley, G. *Am. Mineral* **1963,** 48, 1266.
3. Burley, G. *J. Phys. Chem.* **1964,** 68, 1111.
4. Strock, L. W. *Z. Phys. Chem.* **1934,** 25, 441.
5. Tubandt, C.; Lorenz, E. *Z. Phys. Chem.* **1914,** 87, 513, 543.
6. Perrott, C. M.; Fletcher, N. H. *J. Chem. Phys.* **1968,** 48, 2143.

7. Perrott, C. M.; Fletcher, N. H. *J. Chem. Phys.* **1968,** 48, 2681.
8. Perrott, C. M.; Fletcher, N. H. *J. Chem. Phys.* **1969,** 50, 2770.
9. Perrott, C. M.; Fletcher, N. H. *J. Chem. Phys.* **1970,** 52, 3368.
10. Perrott, C. M.; Fletcher, N. H. *J. Chem. Phys.* **1970,** 52, 3373.
11. Jost, W. *J. Chem. Phys.* **1971,** 55, 4680.
12. Lieser, K. H. *Z. Phys. Chem. N.F. (Frankfurt)* **1954,** 2, 238.
13. Hoshino, S. *J. Phys. Soc. Jpn* **1957,** 12, 315.
14. Jost, W.; Oel, H. J.; Schniedermann, G. *Z. Phys. Chem. N.F. (Frankfurt)* **1958,** 17, 175.
15. Nölting, J. *Ber. Bunsenges. Phys. Chem.* **1963,** 67, 172.
16. Nölting, J.; Rein, D. *Z. Phys. Chem. N.F. (Frankfurt)* **1969,** 66, 150.
17. Nernst, W.; Schwers, F. *Sitzber. kgl. Preuss. Akad. Wiss.* **1914,** 355; *Ann. Physik* **1911,** 36, 395.
18. Pitzer, K. S. *J. Am. Chem. Soc.* **1941,** 63, 516.
19. Madison, M. R.; LeDuc, H. G.; Coleman, L. B. *J. Chem. Phys.* **1984,** 81, 470 (See also LeDuc, H. G.; Coleman, L. B. *Solid State Ionics* **1981,** 5, 469.)
20. Perrott, C. M.; Fletcher, N. H. *J. Chem. Phys.* **1969,** 50, 2344.
21. Grønvold, F.; Westrum, E. F., Jr. *J. Chem. Thermodynamics* **1986,** 18, 381.
22. Okazaki, H.; Takano, A. *Z. Naturforsch., A: Phys., Phys. Chem., Kosmophys.* **1985,** 40A(10), 986.
23. Allen, P. C.; Lazarus, D. *Phys. Rev. B* **1978,** 17, 1913.
24. Fontana, A.; Mariotto, G.; Fontana, M. P. *Phys. Rev. B* **1980,** 21, 1102.
25. Mariotto, G.; Fontana, A.; Cazzanelli, E.; Rocca, F.; Fontana, M. P.; Mazzacurati, V.; Signorelli, G. *Phys. Rev. B* **1981,** 23, 4782.
26. Tallon, J. *Phys. Rev. Lett.* **1986,** 57, 2427.
27. Börjesson, L.; Torell, L. M. *Solid State Ionics* (in press).
28. Mazzacurati, V.; Ruocco, G.; Signorelli, G.; Cazzanelli, E.; Fontana, A.; Mariotto, G. *Phys. Rev. B* **1982,** 26, 2216.
29. Lawn, B. R. *Acta Cryst.* **1964,** 17, 1341.
30. Szabó, G. *J. Phys. C: Solid State Phys.* **1986,** 19, 3775.
31. Szabó, G.; Kertész, J. *J. Phys. C: Solid State Phys.* **1986,** 19, L273.
32. Henisch, H. K. *Crystal Growth in Gels.* Pennsylvania State University Press: University Park, PA. **1970.**
33. Suri, S. K.; Henisch, H. K.; Faust, J. W. *J. Cryst. Growth* **1970,** 7, 277.
34. Deslattes, R. D.; Henins, A. *Phys. Rev. Lett.* **1973,** 31, 972.
35. Ersson, N. O. Personal communication.
36. Burley, G. *J. Chem. Phys.* **1963,** 38, 2807.
37. Chateau, H.; de Cugnac, A.; Pouradier, J. *Compt. Rend. (Paris)* **1964,** 258, 1548.
38. Wilman, H. *Proc. Phys. Soc. London* **1940,** 52, 323.
39. Burley, G. *J. Phys. Chem. Solids* **1964,** 25, 629.
40. Berry, C. R. *Acta Cryst.* **1949,** 2, 393.
41. Yvon, K.; Jeitschko, W.; Parthé, E. *J. Appl. Crystallography* **1977,** 10, 73.
42. Cava, R. J.; Reidinger, F.; Wuensch, B. J. *J. Solid State Comm.* **1977,** 24, 411.
43. Westrum, E. F., Jr.; Furukawa, G. T.; McCullough, J. P. *Experimental Thermodynamics, Vol. I.* McCullough, J. P.; Scott, D. W.: editors. Butterworth: London. **1968,** p. 133.
44. Saito, K.; Atake, T.; Chihara, H. *J. Chem. Thermodynamics* **1987,** 19, 633.
45. Inaba, A. *J. Chem. Thermodynamics* **1983,** 15, 1137.
46. Inaba, A.; Fujii, H.; Chihara, H. To be published.
47. Grønvold, F. *Acta Chem. Scand.* **1967,** 21, 1695.
48. Nölting, J. Personal communication. **1984.**
49. Avogadro, A.; Dworkin, A.; Ferloni, P.; Ghenfentein, M.; Magistris, A.; Szwarc, H.; Toscani, S. *J. Non-cryst. Solids* **1983,** 58, 2–3.
50. Helmholz, L. *J. Chem. Phys.* **1935,** 3, 740.
51. Bührer, W.; Nicklow, R. M.; Brüesch, P. *Phys. Rev. B* **1978,** 17, 3362.
52. Komada, N.; Westrum, E. F., Jr. To be published.
53. Singh, D.; Varshni, Y. P. *Phys. Rev. B* **1981,** 24, 4340.
54. Lieser, K. H. *Z. Phys. Chem. N.F. (Frankfurt)* **1955,** 5, 125.
55. Davis, B. L.; Blair, D. N. *J. Geophys. Res.* **1968,** 73, 6019.
56. Fjeldly, T. A.; Hanson, R. C. *Phys. Rev. B* **1974,** 10, 3569.
57. Weiss, K. *Z. Phys. Chem. N.F. (Frankfurt)* **1968,** 59, 318.
58. Yamada, Y. Dissertation, University of Göttingen, Physical Chemistry Institute. **1958.**
59. Börjesson, L. Dissertation, Department of Physics, Chalmers University, Sweden. **1987.**
60. Börjesson, L.; Torell, L. M. *Phys. Rev. B.* **1987,** 36, 4915.

61. Shahi, K.; Weppner, W.; Rabenau, A. *Phys. stat. sol. (a)* **1986,** 93, 171.
62. Shahi, K.; Wagner, J. B., Jr. *Phys. Rev. B* **1981,** 23, 6417.
63. Strock, L. W. *Z. phys. Chem. B* **1936,** 31, 132.
64. Bührer, W.; Hälg, W. *Helv. Phys. Acta* **1974,** 47, 27.
65. Hoshino, S.; Sakuma, T.; Fujii, Y. *Solid State Comm.* **1977,** 22, 763.
66. Boyce, J. B.; Hayes, T. M.; Stutius, W.; Mikkelsen, J. C., Jr. *Phys. Rev. Lett.* **1977,** 38, 1362.
67. Beyeler, H. U.; Bruesch, P.; Pietronero, L.; Schneider, W. R.; Strassler, S.; Zeller, H. R. *Superionic Conductors. Topics in Current Physics 15.* Salamon, M. B.: editor. Springer-Verlag: Berlin. **1979,** p. 77.
68. Bellati, M.; Romanese, R. *Phil. Trans. Roy. Soc. London* **1882,** 173, 1169.
69. Mallard, E.; Le Chatelier, H. *Bull. Soc. Min. France* **1883,** 6, 181; *Compt. Rend (Paris)* **1883,** 97, 102.
70. Bridgman, P. W. *Proc. Am. Acad Arts Sci.* **1915,** 51, 55.
71. Cohen, E.; Joss, E. J. *J. Am. Chem. Soc.* **1928,** 50, 727.
72. Hennicke, H. Dissertation, Halle a.d.S. **1938,** p. 17.
73. Majumdar, A. J. Dissertation, Pennsylvania State University, University Park. **1958,** p. 152.
74. Majumdar, A. J.; Roy, R. *J. Phys. Chem.* **1959,** 63, 1858.
75. Rao, K. J.; Rao, C. N. R. *J. Mater. Sci.* **1966,** 1, 23.
76. Berger, C.; Raynaud, R.; Richard, M.; Eyraud, L. *Compt. Rend. B (Paris)* **1967,** 265, 716.
77. Carré, J.; Pham, H.; Rolin, M. *Bull. Soc. Chim. France* **1969,** 2322.
78. Natarajan, M.; Rao, C. N. R. *J. Chem. Soc. A.* **1970,** 3087.
79. Mellander, B.-E.; Baranowski, B.; Lundén, A. *Phys. Rev. B* **1981,** 23, 3770.
80. Quaranta, N. E.; Bazán, J. C. *Solid State Ionics* **1983,** 11, 71.
81. Jost, W. *Diffusion in Solids, Liquids, and Gases.* Academic Press: New York. **1960,** p. 95.
82. Shapiro, S. M.; Feidinger, F. *Physics of Superionic Conductors.* Salamon, M. B.: editor. Springer-Verlag: Berlin, Heidelberg. **1979,** p. 45.
83. Huberman, B. A.; Martin, R. M. *Phys. Rev. B* **1976,** 13, 1498.